# DETAILED MODELING OF SEEDED FREE-ELECTRON LASERS

S. Reiche – Paul Scherrer Institute, Villigen, Switzerland
M. Carlà – Università degli Studi di Firenze, Florence, Italy

*Abstract*

Seeding schemes for Free Electron Lasers have mostly a strong impact on the electron distribution by either a conversion of an energy modulation into a current modulation with high harmonic content (HGHG seeding) or an overcompression of this energy modulation to induce energy bands (EEHG seeding) or smear out any bunching in the electron beam (self-seeding).

Most codes follow an approach using thin electron slices, which are carefully generated to provide the correct shotnoise but which also prevents them from mixing and resorting the macro-particle distribution. The FEL code Genesis 1.3 has been modified to allow resolution of each individual electron. Using this approach the correct shot noise at all frequencies is provided and permits re-binning of the particles to the 3D radiation grid at any time. The results for self-seeding and HGHG seeding are discussed.

## INTRODUCTION

Most FEL programs, such as Genesis [1] and Ginger [2], run with less particles than the number of electrons to be simulated for fast and efficient calculations. To simulate the correct shot noise in the electron distribution they rely on quiet loading algorithms [3] to suppress the inherent fluctuation in the macro particle distribution and to randomize the particle positions in a controlled manner. A common approach is to group macro particles into "beamlets" [4], where the group is evaluated as a whole when used in the source term of the Maxwell equation.

However these codes are required to keep these beamlets together at the same grid location of the radiation field. While this is fully sufficient for single pass SASE FEL simulations strong electron beam manipulations can spread electrons over many wavelength. Most prominent are advanced methods such as echo-enabled harmonic generation [5] and the debunching effect in a self-seeding scheme [6]. The beamlets cannot be split, redistributed over the radiation grid and then recombined with other macro particles. Therefore both schemes cannot be modeled self-consistently with the existing codes.

On the other hand it has to be noted that for X-ray FELs the number of electrons per radiation wavelength is relatively low (e. g. a 3 kA beam contains only 1500 electrons per wavelength at 1 Å) and lies within the capability of FEL simulation codes which progress sequentially through the electron beam keeping only a few radiation slices in memory at any time. A direct representation of each individual electron would simplify the preparation of the particle distribution a lot. Therefore Genesis 1.3 has been modified to model all electrons.

This paper describes the simulation strategy to resolve each individual electron in the bunch and the adaptation in the algorithm to sort particles after some radical changes in the particle distribution such as magnetic chicanes or conversion to a higher harmonic. Based on the modified code, sample problems for self-seeding [7] and HGHG FELs [8] are calculated and discussed in the following sections.

## SIMULATION STRATEGY

Because Genesis propagates electron slices sequentially through the undulator the sorting among slices cannot be integrated directly into the source code. Instead the electron distribution is dumped after the first stage and an external program sorts and rebins the electrons to generate a new particle file, which is then imported into Genesis for the second stage of the FEL. The sorting program utilizes a parallel computer using MPI, which allows to hold the entire particle distribution of about 40 GByte of size in memory. Because the sorting in the longitudinal position is a one dimensional problem the MPI algorithm is structured very similar to the bubble sort algorithm [9]. The very efficient algorithm is briefly described in the following.

All nodes are arranged in a 1D topology, where each node corresponds to a slice in the longitudinal bunch frame. Each node reads a section of the particle distribution and splits them into three distributions: particles which are located ahead of the given time-window, particles behind the time window and particles which fall into the time-window. The particles, which are not in the correct time window, are then exchanged with adjacent nodes, pushing them in the correct direction within the 1D topology. Each node gathers particles from two neighbor nodes and the sorting process is repeated until each node indicates that no more electrons need to be transmitted. Then each node bins the electrons within its time-window into the individually radiating slices and writes out the particle distribution.

It is foreseen that in a future release Genesis will hold the entire particle distribution in memory. Then the algorithm, described above, can be integrated into the code for a single execution of a multi-stage FEL.

## SELF-SEEDING

The simulations for self-seeding are modeled after the layout of the SwissFEL hard X-ray FEL beamline Aramis

ISBN 978-3-95450-123-6

[10], using a diamond crystal to generate the seed signal of the second stage. The electron bunch has a charge of 10 pC, a peak current of 1.5 kA, an RMS energy spread of 350 keV and a slice emittance of 0.15 mm mrad. For the studies in this paper we simplified the effect of the crystal and replaced the radiation input of the second stage with a constant seed of 1 MW. This allows us to see the effects from the beam transport more clearly.

### *Shot Noise in the Second Stage*

All self-seeding models assume that the chicane after the first stage removes any induced bunching and that the bunch can be considered fresh when entering the second stage. The effect of a chicane with an $R_{56} = 16\ \mu$m is shown in Fig. 1. The current bunching profile at the exit of the first stage (blue curve) is significantly reduced at the entrance of the second stage (red curve) and any visible coherence over the cooperation length of about 100 nm is removed.

Table 1: Fluctuation of the Bunching at Entrance of Second Stage for Various Length of First Stage

| 1st stage | $< \|b\|^2 >$ | $\sqrt{< \Delta\|b\|^2 >}$ |
|---|---|---|
| 5 modules | $3.20 \cdot 10^{-4}$ | $3.20 \cdot 10^{-4}$ |
| 6 modules | $3.19 \cdot 10^{-4}$ | $3.19 \cdot 10^{-4}$ |
| 7 modules | $3.26 \cdot 10^{-4}$ | $3.31 \cdot 10^{-4}$ |

For a truly fresh bunch the fluctuation in the bunching is given by the number of electrons $n$ per wavelength with $< |b|^2 >= 1/n$ and $\sqrt{< \Delta|b|^2 >} = 1/n$. In the case considered the number of electrons is $n = 3125$. Table 1 lists the mean values and standard deviation at the beginning of the second stage for different number of modules in the first stage.

The removed bunching corresponds quite well to the properties of a fresh bunch. Only for 7 modules in the first stage a slight enhancement is noticeable, which is only visible if the particles are sorted before being injected into the second stage. In this case the first stage exhibits saturation effects already and electrons are pushed by up to 50 wavelengths due to the $R_{56}$ of the chicane.

Figure 1: Bunching at exit of first stage and entrance of second stage (blue and red line, respectively).

### *FEL Performance*

The performance of the self-seeded FEL is shown in Fig. 2 for different lengths of the first stage. A length of 7 modules brings the first stage close to saturation. Each module less reduces the extracted power of the first stage by a factor of about 5.4. The growth of a SASE FEL has been superimposed in the plot but shifted in longitudinal position for better comparison of the growth rates.

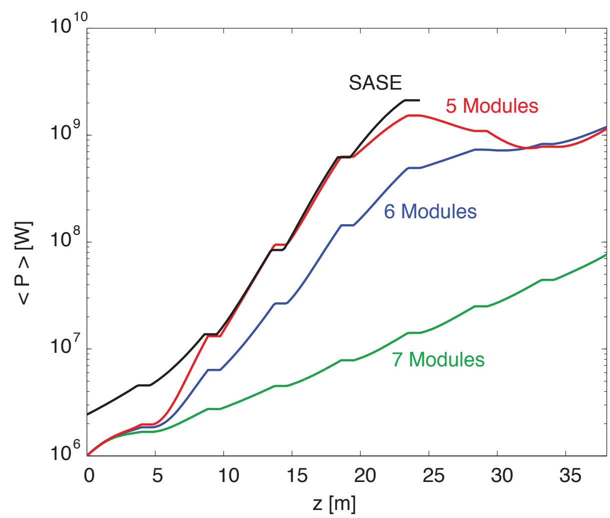


Figure 2: FEL power along the second stage for various lengths of the first stage. The SASE performance has been shifted in position for better comparison.

The operation with only 5 modules in the first stage – namely extracting at a power level 30 times less than the saturation power – shows no difference in the growth rate for the second stage. However any longer first stage has the penalty that the growth rate in the second stage is reduced. This is caused by the induced energy spread of the SASE process in the first stage beyond a level where it affects the FEL performance in the succeeding stage. However it is remarkable that even a beam, which has reached saturation, can amplify a seed signal (see green curve in Fig. 2). This amplification is driven by slices of the electron beam, which are located between spikes of the SASE process in the first stage. The quality of these slices is sufficient for FEL amplification.

Although the seed is fully coherent and the local bunching has been reduced to the shot noise level an echo effect of the SASE profile is carried over into the second stage. Instead of being flat the profiles at saturation are spiky and very similar to a SASE pulse. However all those spikes are correlated in phase and the spectrum is significantly nar-



ISBN 978-3-95450-123-6

rower than a SASE spectrum. When comparing the bunching at the end of the first stage (blue curve in Fig. 1) with the radiation profile (blue curve in Fig. 3) the spikes in the bunching correlate strongly with the gaps in the radiation profile.

This modulation in the profile is caused by the modulation of the electron bunch in energy and energy spread with a characteristic scale of the SASE cooperation length. The $R_{56}$ of the chicane is sufficient to remove the bunching but isn't strong enough to wash out the energy modulation. For the case of 6 modules in the first stage the average power is well below saturation power but the peaks of the SASE spikes exhibit larger amplitudes and can reach, in their peak values, the saturation power level. The electrons at those spike locations have been shifted away in energy from the resonant condition and suffer reduced growth rates in the second stage due to detuning effects [11]. Hence the appearance of holes in the radiation profile even in the case of a perfectly coherent seed signal. This imposes a limitation on any post-saturation tapering [12] because the variation in the radiation amplitude causes detrapping of the electrons in the radiation field bucket when the field slips along the bunch and the growth in the radiation field stops.

As for any FEL amplifier the performance of the FEL can be enhanced by applying a detuning and taper to the undulator field of the second stage. In particular the average energy loss of the SASE FEL process in the first stage needs to be compensated by preserving the resonant condition. It works in particular well for the case of 7 modules, where almost the entire electron bunch is shifted out of the FEL resonant bandwidth. The enhancement in the radiation power at the undulator exit is about a factor of 10, while it is about a factor of 3 and 2 for 6 and 5 modules, respectively.

## HIGH GAIN HARMONIC GENERATION

Harmonic generation, such as the HGHG and the Echo-enabled Harmonic Generation (EEHG), are difficult to model because it requires changing the longitudinal resolution in the conversion process. The ideal solution would be to rebin the electron distribution into the radiation slices of the higher harmonics. The internal degrees of freedom in the macro particle distribution, expressing the bunching at the higher harmonics (e.g. $b_n$ for the $n$th harmonics), need to be transformed into fundamental bunching factors at the harmonic wavelength (e.g. $n$ samples of $b_1$ to cover the same length scale) when slicing the distribution. The problem is typically avoided by keeping the same sampling rate as the fundamental wavelength and treating the particle distribution as the average over $n$ slices [13].

Figure 3: Radiation profile at saturation for 5, 6, and 7 module in the first stage (red, blue and green line, respectively).

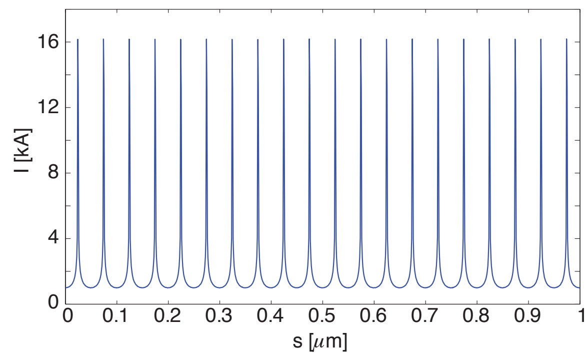


Figure 4: Current profile for a HGHG seed signal of 50 nm, converted to 1 nm.

A related problem is that in this approach slices do not mix. This is in particular a problem for echo-enabled harmonic generation, where in the harmonic process electrons are shifted by many wavelengths of the fundamental signal. Studies such as jitter in the drive laser amplitude and phase become impossible to model.

As in the self-seeding simulation the problem is trivialized when all electrons are represented. The particle distribution can easily be sliced into finer slices during the conversion process. The bunching and the current is resolved on a finer scale as shown in Fig. 4 for a harmonic conversion to the 50th harmonic.

The HGHG simulations use a continuous beam with a current of 2 kA and then transmitted through a chicane to convert to the final harmonic of 1 nm. The current profile exhibits strong current spikes above 10 kA while a lot of slices have a beam current of around 1 kA. The coherent radiation field from the spikes slips from one current spike to the next over 50 undulator periods while imprinting its signal onto the lower current part between the spikes. It seems intuitive that the FEL should amplify the radiation with an effective current much less than 2 kA. However the growth of the radiation field (red curve in Fig. 5) agrees quite well with the standard solution of averaging over 50 slices (blue curve) with an average current of 2 kA. A lower current (green dashed line) differs significantly from the detailed simulation.

While no significant difference is found between the established methods and the more exact approach, presented here, the one-one simulation allows for other studies, such as phase tolerances in EEHG simulations. One aspect, which hasn't been included in the simulation is the effect of the longitudinal space charge arising from the huge current spikes in the HGHG process. This might impose a practical limit in the HGHG process, which cannot be modeled in the 'slice-average' methods.

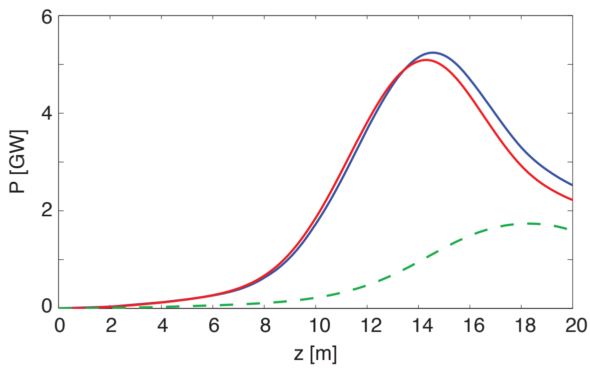


Figure 5: Time-dependent simulation of the second stage in a HGHG configuration, operating at the 50th harmonics (red curve). For comparison the slice-averaged results are shown for nominal current (blue curve) and reduced current (green dashed line).

## ECHO-ENABLED HARMONIC GENERATION

We applied the capability of resolving each individual electron to simulate seeded FELs based on echo-enabled harmonic generation [5]. In contrast to HGHG, where the electrons are typically kept within the same slice of the seeding wavelength, EEHG applies a more violent mixing of electrons among different slices. The current solution of folding the macro particles back into the same slice [14] might work but imposes some severe limitations. Studies such as phase and amplitude variation in the seed signal cannot be done with the standard approach.

Instead of sorting the particles after the first stage of a multi stage FEL (see sections above) we decided for the sake of simplicity to generate directly the phase space distribution in a Monte-Carlo approach of rejection and acceptance. We randomly select a coordinate in the longitudinal phase space and transforms the coordinates back to its original position before the first modulator of the EEHG seeding section. There we evaluate the probability in the density function and compared it with a random number from a uniform distribution. If the random number is smaller than the probability the particle location will be accepted to fill the phase space distribution.

We used the same beam parameters as in the HGHG simulation but for a conversion from 250 nm to 1 nm. In this ideal EEGH configuration we observed several effects: First, the bunch profile is elongated due to the large value of energy modulation and $R_{56}$ of the chicanes. Second, neighbor harmonics fall also within the FEL bandwidth and are amplified as well. Third, the effective spacing between bunched slices is longer than the slippage over one gain length. The FEL profile exhibits superradiant features, rising to larger peak values of up to 20 GW, about 5 times larger than the saturation level of an FEL with a perfectly monochromatic seed. Extensive studies will follow to analyze the impact of amplitude and phase error in the seed signal and the operation with seed pulses shorter than the electron bunch.

## CONCLUSION

With the growing capacity and execution speed of modern computers the number of macro particles can be increased till each electron in the bunch is resolved. This trivializes the problem of the shot noise and other limitations in FEL codes, preventing macro particles to be redistributed after they have moved out of the time window of a given radiation slice. This allows for a higher degree of modeling, in particular for advanced schemes such as EEHG, HGHG and self-seeding, which are pushing the limits of most time-dependent codes, which were developed mostly for single pass SASE FELs.

As typical example using this extended ability of modeling, the paradigm that a magnetic chicane refreshes the electron distribution is not fully valid for all aspects. While the local bunching is indeed washed out the residual variations in energy and energy spread yield a spiky radiation profile despite having a fully coherent seed signal. While the impact on the spectral brightness is negligible it imposes a limitation for any post-saturation taper mechanism to enhance the efficiency of the FEL.

## REFERENCES

[1] S. Reiche, Nucl. Instr. & Meth. **A 429** (1999) 243.

[2] W.M. Fawley, LBNL-49625-Rev. I (2004).

[3] C. Penman and B.W.J. McNeil, Opt. Comm. **80** (1992) 82.

[4] W.M. Fawley, Phys. Rev. STAB **5** (2002) 070701.

[5] D. Xiang and G. Stupakov, Phys. Rev. STAB **12** (2009) 030702.

[6] J. Feldhaus, *et al*, Opt. Comm. **140** (1997) 341.

[7] G. Geloni, V. Kocharyan and E. Saldin, *Scheme for generation of highly monochromatic X-rays from a baseline XFEL undulator*, DESY 10-033 (2010).

[8] L.H. Yu, Phys. Rev. **A 44**, 5178(1991).

[9] W.H. Press *et al*, *Numerical Recipes in Fortran 77* (Cambridge University Press, Cambridge,1992).

[10] R. Ganter *et al*, PSI-Bericht 10-04.

[11] R. Bonifacio *et al*, Opt. Comm. **50**(1984) 373.

[12] Y. Jiao *et al*, Phys. Rev. STAB **15** (2012) 050704

[13] L.H. Yu *et al*, Science **11**(2000) 932.

[14] Z.T. Zhao *et al*, Nature Photonics **6** (2012) 360-363.



ISBN 978-3-95450-123-6